Spectrochimica Acta Part A: Molecular and Biomolecular Spectroscopy 116 (2013) 122–131

Contents lists available at SciVerse ScienceDirect

Spectrochimica Acta Part A: Molecular and Biomolecular Spectroscopy

journal homepage: www.elsevier.com/locate/saa

Layered crystal structure, conformational and vibrational properties of 2,2,2-trichloroethoxysulfonamide: An experimental and theoretical study

Diego M. Gil [a], Oscar E. Piro [b,1], Gustavo A. Echeverría [b,1], María E. Tuttolomondo [a], Aída Ben Altabef [a,*,1]

[a] INQUINOA, CONICET, Instituto de Química Física, Facultad de Bioquímica, Química y Farmacia, Universidad Nacional de Tucumán, San Lorenzo 456, T4000CAN Tucumán, Argentina
[b] Departamento de Física, Facultad de Ciencias Exactas, Universidad Nacional de La Plata and Institute IFLP (CONICET, CCT-La Plata), C.C. 67, 1900 La Plata, Argentina

HIGHLIGHTS

- The molecular structure of the compound has been determined by X-ray diffraction.
- The substance crystallizes in the monoclinic $P2_1/c$ space group with $Z = 8$ molecules per unit cell.
- The conformers are arranged in the lattice as center-symmetric N—H···O(sulf) bonded dimers.
- For NBO analysis, the hyperconjugative interactions are favored in conformer 2 than conformer 1.
- Infrared and Raman spectra showed bands assignable to 34 of the 36 vibrational normal modes.

GRAPHICAL ABSTRACT

Crystal packing of $Cl_3CCH_2OSO_2NH_2$ showing the $CCl_4\cdots Cl_4C$ Van der Waals interaction and the molecular structure of both conformers 1 and 2 obtained by single crystal DRX measurements.

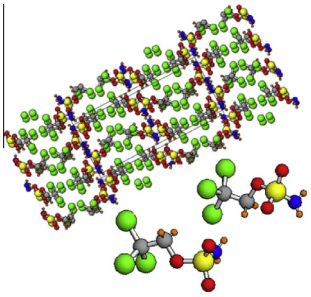

ARTICLE INFO

Article history:
Received 3 May 2013
Received in revised form 4 July 2013
Accepted 8 July 2013
Available online 18 July 2013

Keywords:
Crystal X-ray diffraction structure
Ab initio MO calculations
Natural bond orbital analysis
Infrared and Raman spectroscopy

ABSTRACT

The molecular structure of 2,2,2-trichloroethoxysulfonamide, $CCl_3CH_2OSO_2NH_2$, has been determined in the solid state by X-ray diffraction data and in the gas phase by ab initio (MP2) and DFT calculations. The substance crystallizes in the monoclinic $P2_1/c$ space group with $a = 9.969(3)$ Å, $b = 22.914(6)$ Å, $c = 7.349(2)$ Å, $\beta = 91.06(3)°$, and $Z = 8$ molecules per unit cell. There are two independent, but closely related molecular conformers in the crystal asymmetric unit. They only differ in the angular orientation of the sulfonamide ($—SO_2NH_2$) group. The conformers are arranged in the lattice as center-symmetric N—H···O(sulf)-bonded dimers. Neighboring dimers are linked through further N—H···O(sulf) bonds giving rise to a crystal layered structure. The solid state infrared and Raman spectra have been recorded and the observed bands assigned to the molecular vibration modes. Also, the thermal behavior of the substance was investigated by TG–DT analysis. The stability of the molecule arising from hyper-conjugative interactions and charge delocalization has been analyzed using natural bond (NBO) analysis.

Introduction

The introduction of sulfonamides into clinical medicine in the 1930s marked the beginning of microbial chemotherapy. Sulfonamides are an important kind of pharmaceutical compounds that currently exhibit a wide spectrum of antibacterial, diuretics, hypoglycemic and HIV protease inhibiting biological activities [1]. The emerging resistance of microorganisms to some synthetic pharmaceuticals makes it necessary to continue the search for new antimicrobial substances. Numerous molecules containing a sulfonamide structure have been synthesized, including aromatic sulfonamides that inhibit the growth of tumor cells [2]. Because of the

* Corresponding author. Tel.: +54 381 4311044; fax: +54 381 4248169.
E-mail address: altabef@fbqf.unt.edu.ar (A.B. Altabef).
[1] Members of the Carrera del Investigador Científico, CONICET, Argentina.

1386-1425/$ - see front matter © 2013 Elsevier B.V. All rights reserved.
http://dx.doi.org/10.1016/j.saa.2013.07.013

wide variety of the biological importance of the sulfonamides, the synthesis of several substituted sulfonamides, the study of their crystal structure and other physical, chemical and biochemical studies have become interesting fields in research.

The availability and stability of sulfonamides esters make them particularly attractive reagents for different processes such as amine synthesis through intermolecular C—H amination using as Rh-based catalyst, which was reported by Willians Fiori and Du Bois [3]. This process is possible due to the fact that sulfonanides esters are an excellent nitrogen source. Xu et al. have reported the arizidination of olefins catalyzed by N-heterocyclic carbene copper complexes and 2,2,2-trichloroethoxysulfonamide, $CCl_3CH_2OSO_2NH_2$ as a nitrogen source [3,4]. This compound, derived from an aliphatic alcohol, was more efficient in the reaction.

In this work we report the crystal structure of $CCl_3CH_2OSO_2NH_2$ by X-ray diffraction methods and its infrared, Raman and NMR spectra. The thermal behavior of the substance has also been studied by TG–DT analysis. These experimental measurements were complemented by quantum chemical calculations to obtain an optimized molecular structure and a scaled quantum mechanical force field. Based on the comparison with related molecules and assisted by the theoretical results, the spectral features were subsequently assigned to the different normal modes of vibration. The study was complemented by natural bond orbital (NBO) analysis to assess the significance of hyper-conjugative interactions, which could favor one conformation over another.

Experimental

Samples of $CCl_3CH_2OSO_2NH_2$ for use in both X-ray diffraction and spectroscopy experiments were purchased from Sigma–Aldrich and used without further purification. Adequate single crystals for structural X-ray diffraction measurements were obtained from slow evaporation at 20 °C of concentrated chloroform solutions.

X-ray diffraction data

The measurements were performed on an Oxford Xcalibur Gemini, Eos CCD diffractometer with graphite-monochromated Mo Kα (λ = 0.71073 Å) radiation. X-ray diffraction intensities were collected (ω scans with ϑ and κ-offsets), integrated and scaled with the CrysAlisPro suite of programs [5]. The unit cell parameters were obtained by least-squares refinement (based on the angular settings for all collected reflections with intensities larger than seven times the standard deviation of measurement errors) using CrysAlisPro. Data were corrected empirically for absorption employing the multi-scan method implemented in CrysAlisPro. The structure was solved by direct methods with SHELXS-97 [6,7] and the molecular model refined by full-matrix least-squares procedure on F^2 with SHELXL-97 [8,9]. All hydrogen atoms were located in a difference Fourier map and refined at their found positions with isotropic displacement parameters. The N—H distances were restrained to a target value of 0.87(1) Å. Crystal data and structure refinement results are summarized in Table 1. Crystallographic structural data have been deposited at the Cambridge Crystallographic Data Centre (CCDC). Any request to the Cambridge Crystallographic Data Centre for this material should quote the full literature citation and the reference number CCDC 900580.

IR and Raman spectroscopy

The infrared absorption spectrum of $CCl_3CH_2OSO_2NH_2$ was zrecorded in KBr pellets within the 4000–400 cm^{-1} range using a Perkin-–Elmer GX1 FTIR instrument and the Raman dispersion spectrum of the solid was measured in the 3500 and 50 cm^{-1} interval with a Thermoscientific DXR Raman microscope. The Raman data were collected using a diode-pump, solid state laser of 532 nm (5 cm^{-1} spectral resolution), a confocal aperture of 25 μm pinhole, and a 10× objective. The sample was placed on gold-coated sample slides. To achieve a sufficient signal to noise ratio, 30 expositions of 2 s each were accumulated during the measurements with the laser power maintained at 10 mW.

Table 1
Crystal data and structure refinement results for 2,2,2 trichloroethoxysulfonamide.

Empirical formula	$C_2H_4Cl_3NO_3S$
Formula weight	228.47
Temperature	568(2) K
Wavelength	0.71073 Å
Crystal system	Monoclinic
Space group	$P2_1/c$
Unit cell dimensions	a = 9.969(3) Å b = 22.914(6) Å c = 7.349(2) Å β = 91.06(3)°
Volume	1678.4(8) $Å^3$
Z	8
Density (calculated)	1.808 Mg/m^3
Absorption coefficient	1.291 mm^{-1}
$F(000)$	912
Crystal size	0.64 × 0.35 × 0.03 mm^3
θ – range for data collection	3.36–26.00°
Index ranges	$-12 \leqslant h \leqslant 12$, $-28 \leqslant k \leqslant 20$, $-8 \leqslant l \leqslant 9$
Reflections collected	9614
Independent reflections	3279 [R(int) = 0.0551]
Observed reflections [$I > 2\sigma(I)$]	2219
Completeness to ϑ = 26.00°	99.5%
Max. and min. transmission	0.9574 and 0.4916
Refinement method	Full-matrix least-squares on F^2
Data/restraints/parameters	3279/4/213
Goodness-of-fit on F^2	1.051
Final R indices [$I > 2\sigma(I)$]	$R1$ = 0.0510, wR_2 = 0.1189
R indices (all data)	$R1$ = 0.0810, wR_2 = 0.1468
Largest diff. peak and hole	0.695 and −0.512 $eÅ^{-3}$

^1H and ^{13}C NMR measurements

The ^1H and ^{13}C NMR spectra of the compound were recorded at 298 K on a Bruker spectrometer. The substance was dissolved in $CDCl_3$ and the resulting solution introduced into a 5 mm NMR tube. Chemical shifts, δ, for ^{13}C and ^1H NMR spectra are given in parts per million relative to tetramethylsilane (TMS; δ = 0 ppm) and are referenced by using the residual non-deuterated solvent signal.

Thermal analysis

Thermogravimetric (TGA) and differential thermal (DTA) measurements were performed with a Shimadzu TGA-50 and DTA-50 units in the temperature range from 20 to 500 °C at a heating rate of 5°/min under flowing air.

Quantum chemical calculations

Calculations were performed using the resources of the UK National Service for Computational Chemistry Software (NSCCS) [10] running the Gaussian 03 suite of programs [11]. Geometry optimizations were performed at MP2 [12] and DFT levels using a variety of basis sets. Electron correlation was then considered using the MP2 approach with the 6-311G(d,p), 6-311++G(d,p) and 6-311++G(3df,3pd) basis set [13–16]. DFT calculations were performed using Becke's three-parameter hybrid exchange functional [17] (B3) combined with both the Lee–Yang–Parr

gradient-corrected correlation functional [18] (LYP) and the same basis sets as for the MP2 calculations. The second DFT method used, mPW1PW91 [19] applies a modified Perdew–Wang exchange functional and Perdew–Wang 91 correlation functional [19]. All calculations were performed using standard gradient techniques and default convergence criteria.

A natural bond orbital (NBO) calculation was performed using the NBO 3.1 program [20], as implemented in the Gaussian 03 package, at the B3LYP/6-311++G(d,p) level in order to understand various second order interactions between the filled orbitals of one subsystem and vacant orbitals of another subsystem, with the aim of having a measure of the intra-molecular delocalization of hyper-conjugation. In addition, an analysis of the reactivity of the compound was done within Bader's atoms in molecules theory (AIM) by using the AIM2000 code [21,22].

The calculation of force constants for $CCl_3CH_2OSO_2NH_2$ included force field transformation, scaling and determination of the potential energy distribution (PED), all of which were performed using the FCARTP program [23]. The atomic displacements given by the Gaussian 03 program for each vibrational mode were used to understand qualitatively the nature of the molecular vibrations and, for that purpose, the corresponding data were represented graphically using the GaussView program [24].

Results and discussion

Structural X-ray diffraction

The substance crystallizes in the monoclinic $P2_1/c$ space group with $a = 9.969(3)$ Å, $b = 22.914(6)$ Å, $c = 7.349(2)$ Å, $\beta = 91.06(3)°$, and $Z = 8$ molecules per unit cell. There are two 2,2,2-trichloroethoxysulfonamide molecular conformers in the crystal asymmetric unit. They are shown in the ORTEP [25] view of Fig. 1. The representation of the crystal packing is shown in Fig. 2. The corresponding bond distance and angles are listed in Table S1 and S2 (Supporting information). The molecules only differ in the conformational orientation of the sulfonamide ($—SO_2NH_2$) group. In fact, the *rms* separation between homologous non-H atoms (including the sulfur atom) in the best least-squares structural fitting, calculated by the Kabsh's procedure [5], is 0.046 Å. The orientation of the $—SO_2NH_2$ groups is approximately related to each other through a rotation of about 120° around the S—O(ester) bond.

Intra-molecular bond distances and angles conforms the Organic Chemistry rules. In particular, the C—Cl bond lengths are in the range from 1.751(5) to 1.767(4) Å for conformer 1 (C1) and in the 1.754(4) to 1.763(4) Å interval for conformer 2 (C2). As expected from the sp^3 carbons Ci1 ($i = 1,2$) the bonding angles around these atoms are close to the perfect tetrahedral value

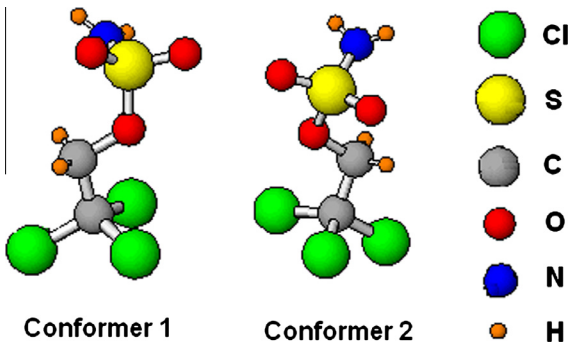

Fig. 1. Molecular structure of conformer 1 and 2 of $CCl_3CH_2OSO_2NH_2$ obtained by single crystal XRD measurements.

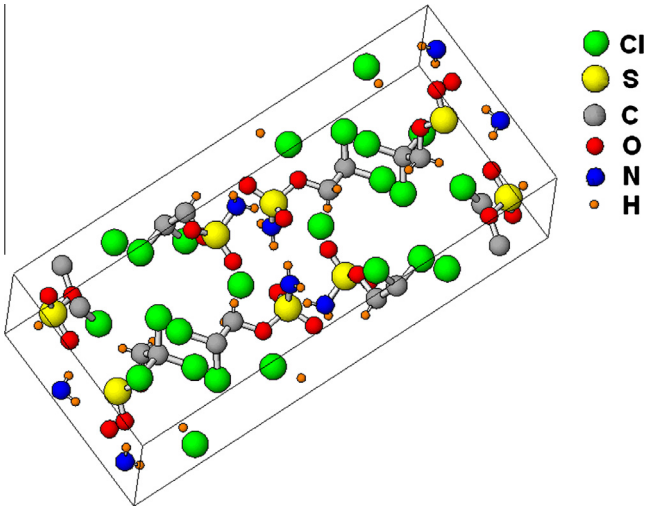

Fig. 2. Crystal packing of $CCl_3CH_2OSO_2NH_2$.

(109.5°): from 107.0(3)° to 111.7(3)° in C1 and from 106.4(3)° to 113.0(3)° in C2.

The $—SO_2NH_2$ groups show the characteristic six valence bonding structure of sulfur, with sulfoxide S=O double bond distances equal to 1.416(4) and 1.419(3) Å for C1 and 1.415(3) and 1.424(3) Å for C2. The single S—N and S—O(ester) bonds lengths are, respectively, 1.571(4) and 1.572(3) Å for C1 and 1.575(4) and 1.572(3) Å for C2. The bonding angles around the sulfur atom depart slightly from tetrahedral value. In fact, the sulfoxide O=S=O angle is 120.1(2)° in C1 and 120.2(2)° in C2, the other angles around sulfur are in the 102.3(2)–110.6(2)° and 101.0(2)–111.8(2)° range for conformers C1 and C2, respectively. All the geometrical parameters obtained by our XRD measurements are in agreement with the values reported for different sulfonamides [26–30].

The conformers of each type are arranged in the lattice as center-symmetric N—H···O-bonded dimers, involving as H-donor the amide group of a given conformer and as acceptor one sulfoxide oxygen atom of a crystallographic inversion-related molecule [N···O bond distances of 3.047 and 2.964 Å for C1 and C2 dimers]. Neighboring dimers of different conformers are linked to each other through inter-dimer N—H···O(sulf) bonds [N···O bond lengths of 2.865 and 3.094 Å] giving rise to a layered structure perpendicular to the unique *b*-axis. The $—CCl_4$ chlorine atoms define the layer surfaces (see Fig. S1). Adjacent layers are bonded to each other through $CCl_4···Cl_4C$ Van der Waals interaction (shortest Cl···Cl contact of 3.533 Å). The H-bonding structure is further detailed in the Supplementary Table S5.

Quantum chemical calculations

Geometrical structures

The optimized structure parameters of the compound were calculated with the MP2 and DFT methods using 6-311G(d,p), 6-311++G(d,p) and 6-311++G(3df,3pd) basis sets. All calculated geometrical parameters obtained by the MP2 and DFT calculations are in good agreement with the experimental structural parameters. The geometric parameters optimized with different basis sets are given in Tables S1 and S2, whereas the molecular models of both conformers appear in Fig. 3. The theoretical results are compared in the same tables with the experimental data resulting from the X-ray diffraction study. Conformer 1 exhibits a C(1)—O(3)—S(6)—N(2) torsion angle of −68° calculated at MP2/6-311++G(3df,3pd) level. This is in agreement with the experimental

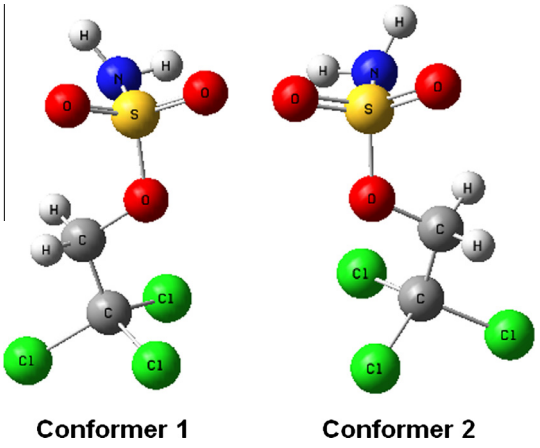

Fig. 3. Geometry optimized structures for both conformers of $CCl_3CH_2OSO_2NH_2$.

value obtained from XRD data (−66.3°). The results of our calculations indicated that the bond lengths S(6)—O(4) and S(6)—O(5) are 1.444 and 1.437 Å, respectively, calculated at MP2 level using the 6-311++G(d,p) basis set. These bond lengths show a typical double bond character and all other distances fall within the expected range. The theoretical description of molecules containing the SO_2 fragment requires the use of highly polarized basis functions. As was found for related compounds such as $CH_3SO_2SCH_3$ [31], $CF_3SO_2OCF_3$ [32] and sulfanilamide [33], the inclusion of extra polarization functions (beyond a single *d*-function) is necessary to predict the bond lengths in these types of molecules accurately. The parameters most sensitive to this orbital description are the S—O and S—N bonds, which were shortened when we replaced the 6-311++G(d,p) basis set with 6-311++G(3df,3pd). All bonds involving the sulfur atom were shortened, but the remaining bond lengths were relatively unchanged. This produced a calculated geometry close to the experimental structure. The S—N bond lengths in C1 and C2 at MP2 and B3LYP levels are 1.639–1.651 and 1.639–1.649 Å, respectively. The MP2 estimates matches well the average (1.571–1.575 Å) distance reported using X-ray crystal data. The longer bond length at the B3LYP level is due to the overestimation of electron–electron repulsions.

For both conformers, the free energy calculated with the B3LYP/6-311G(d,p) method was used along with the average temperature of the experiment to estimate (using the Boltzman distribution) the amount of each conformer that should be observed in the solid state. The calculated free energy difference between both conformers (C1 lower in energy) was 1.37 kJ mol^{-1} and the ratio of C1 to C2 conformers was predicted to be 0.63:0.37.

On the other hand, conformer 2 shows a C(1)—O(3)—S(6)—N(2) torsion angle of 67.6° calculated at MP2 level with 6-311++G(3df,3pd) basis set. Some theoretical values deviate from the corresponding experimental ones; these differences are in principle reasonable considering that the calculations were performed for the molecule in the gas phase, where the intermolecular interactions present in the crystal lattice are not taken into account.

In an attempt to study the behavior of the molecule into the solid state, molecular orbitals (MO) calculations involving two molecules linked through hydrogen bond were carried out at the computationally affordable B3LYP/6-31G(d) level. In our calculations, the hydrogen-bonded model of the dimer was constructed from the X-ray crystal and molecular structure and then the conformation energetically optimized without any constraint to the potential energy surface. The experimental results show a N—H···O bond length of 2.338 Å, a distance close to the experimental value obtained from DXR data. A change in the molecular structure upon dimerization was observed. The N—H and S=O bond lengths increase from 0.862 and 1.419 Å, in the monomer, to 1.026 and 1.466 Å in the dimer, as expected due to the presence of intermolecular hydrogen bonding.

NBO analysis

In order to get some insight into the intra-molecular interactions which justify the relative stability of the 1 and 2 conformers, natural bond orbital (NBO) calculations [20] were performed in both forms of $CCl_3CH_2OSO_2NH_2$. In the NBO analysis, the electronic wavefunction is interpreted as a set of occupied Lewis-type orbitals, paired with a set of formally unoccupied non-Lewis-type orbitals. The electronic interactions within these orbitals, the deviations from the Lewis electronic structure and the delocalization effects can be interpreted as charge transfers between the filled Lewis orbitals (donors) and the theoretically empty non-Lewis orbitals (acceptors). The stabilization energy of these interactions is mainly of the types lone pair (LP) → π^* orbitals (delocalization or mesomeric effect) and LP → σ^* orbitals (hyper-conjugative effect). The results of NBO calculations at the B3LYP/6-311++G(d,p) level on the conformers of $CCl_3CH_2OSO_2NH_2$ appear in Table 2. In terms of NBO analysis, the hyper-conjugative interactions are more favored in conformer 2 than in conformer 1. The lone pair of the nitrogen transfers electronic charge to the anti-bonding σ^* orbital of S—O and S=O bonds. The lone pair LPN(2) in the conformer 1 participates in LPN(2) → σ^* O(3)—S(6) and LP N(2) → σ^* O(5)—S(6) interactions and in conformer 2 participates in LP N(2) → σ^* O(3)—S(6) and LP N(2) → σ^* O(4)—S(6). As seen in Table 2, for the isolated state and in chloroform solution, the hyper-conjugative effect LP N(2) → σ^* O(3)—S(6) is higher in conformer 1 and the LP N(2) → σ^* O(4)—S(6) interaction is more pronounced in conformer 2, while in conformer 1 this interaction is absent. The energy transfer from the lone pairs LPO(3), LPO(4) and LPO(5) to the σ^* N(2)—S(6), σ^* S(6)—O(3) and σ^* S=O is very important for the stability of the conformer 2 in isolated state and in a nonpolar solvent as chloroform.

The relation between the electron occupation of the σ^* S—N orbital and the length of S—N and S—O bonds has been investigated in both conformers. Table 3 shows the S—N and S—O bond lengths with the corresponding electron occupancy of the natural bond orbitals of both conformers of $CCl_3CH_2OSO_2NH_2$. As shown in Table 3, the S—N bond length in conformer 1 is longer than that of conformer 2, which is in agreement with the high occupation of the σ^* S—N in conformer 1 compared with conformer 2. This is in agreement with the higher LP O(3) → σ^* S—N interaction in conformer 1 than in conformer 2 which produces a lengthening of the S—N bond length and a shortening of the S—O bond length.

AIM analysis

The quantum theory of atoms in molecules has been useful in the characterization of bonds through a topological analysis of the electronic charge density and their Laplacian at the Bond Critical Points (BCP) [21]. In the AIM theory the nature of the bonding interaction can be determined through an analysis of the properties of the charge density ρ, and its Laplacian $\nabla^2(\rho)$ at the BCP, and through the properties of the atoms, which are obtained by integrating the charge density over the atomic orbitals [21]. Table 4 shows the bond critical point data for both conformers of $CCl_3CH_2OSO_2NH_2$. As seen in Table 4, the value of the charge density at the S(6)—N(2) bond critical point is relatively high for both conformers 1 and 2 and the Laplacian of electron density is negative hence indicating that the charge density has been concentrated in the inter-nuclear region. Besides, the value of charge density of the S—N bond in conformer 2 is greater than in conformer 1, which leads to

Table 2
Important hyper-conjugative interactions (in kcal mol^{-1}) for $Cl_3CCH_2OSO_2NH_2$ calculated using the B3LYP/6-311++G(d,p) method.

Interaction[a]	Conformer 1		Conformer 2	
	Isolated state	$CHCl_3$ solution	Isolated state	$CHCl_3$ solution
LP N(2) → σ* O(3)—S(6)	6.58	6.49	6.37	6.32
LP N(2) → σ* O(4)—S(6)	–	–	6.59	7.22
LP N(2) → σ* O(5)—S(6)	6.17	7.12	–	–
LP O(3) → σ* N(2—S(6)	7.29	6.94	7.07	6.95
LP O(3) → σ* O(5)—S(6)	2.01	1.96	6.65	6.47
LP O(3) → σ* O(4)—S(6)	6.44	6.48	2.07	1.95
LP O(3) → σ* C(1)—C(12)	0.91	0.84	2.02	0.85
LP O(4) → σ* N(2)—S(6)	23.24	22.49	27.06	26.11
LP O(4) → σ* O(5)—S(6)	22.00	21.44	23.08	22.33
LP O(4) → σ* O(3)—S(6)	32.27	32.18	29.19	28.24
LP O(5) → σ* N(2)—S(6)	26.47	26.08	23.14	22.51
LP O(5) → σ* O(4)—S(6)	23.16	22.37	21.98	21.43
LP O(5) → σ* O(3)—S(6)	29.08	28.27	32.64	32.23

[a] LP denotes electron lone pair on the specified atom.

Table 3
S—N and S—O bond lengths (Å), electron occupancy and energy (kcal mol^{-1}) of the natural bond orbitals for $Cl_3CCH_2OSO_2NH_2$.[a]

	Conformer 1	Conformer 2
r S—N	1.678	1.677
Occupancy σ S—N	1.97606	1.97601
Energy	−0.82381	−0.82466
Occupancy σ* S—N	0.23629	0.23609
Energy	0.08781	0.08894
r S—O	1.630	1.632
Occupancy σ S—O	1.97324	1.97364
Energy	−0.85168	−0.85147
Occupancy σ* S—O	0.30778	0.30975
Energy	0.05067	0.04961

[a] Calculated at the B3LYP/6-311++G(d,p).

Table 4
The B3LYP/6-311++G(d,p) calculated Bond Critical Point (BCP) data and BCP distances (in a.u.) to attractors.

	Conformer 1	Conformer 2
N(2)—S(6)		
ρ	0.2329	0.2332
$\nabla^2(\rho)$	−0.6040	−0.5991
BCP-N(2)	1.8458	1.8520
BCP-S(6)	1.3245	1.3186
d (Å)	1.678	1.677
q N(2)	−0.5143	−0.5116
q S(6)	0.4312	0.3742
S(6)—O(3)		
ρ	0.2174	0.2167
$\nabla^2(\rho)$	−0.1836	−0.1898
BCP-S(6)	1.2337	1.2364
BCP-O(3)	1.8502	1.8504
d (Å)	1.630	1.632
q S(6)	0.4312	0.3742
q O(3)	−0.0694	−0.0807
C(1)—O(3)		
ρ	0.2398	0.2401
$\nabla^2(\rho)$	−0.3682	−0.3706
BCP-C(1)	0.9476	0.9477
BCP-O(3)	1.7639	1.7633
d (Å)	1.434	1.434
q C(1)	−0.9529	−0.9184
q O(3)	−0.0694	−0.0807
C(1)—C(12)		
ρ	0.2525	0.2519
$\nabla^2(\rho)$	−0.6048	−0.6010
BCP-C(1)	1.3783	1.3775
BCP-C(12)	1.5101	1.5135
d (Å)	1.528	1.529
q C(1)	−0.9529	−0.9184
q C(12)	0.9816	1.0041

a decrease in the S—N bond length. The value of charge density at S(6)—O(3) bond critical point in conformer 1 is slightly greater than in conformer 2 and the Laplacian of charge density of both conformers is negative. In this case, the S—O bond length in conformer 2 is greater than conformer 1. These results are in agreement with the NBO analysis which shows that LP O(3) → σ* S(6)—N(2) interaction is more important in conformer 1 thus producing a lengthening of the S—N bond and a shortening of the S—O bond as compared with that of conformer 2.

NMR spectroscopy

The ^{1}H NMR spectrum of the compound in solution was measured to support the structural assignment. Two signals are observed; the one located at 4.74 ppm (singlet) is assigned to protons of the methylene group while the broad one (singlet) observed at 5.31 ppm corresponds to the hydrogen atoms of the sulfonamide moiety.

In the ^{13}C NMR spectrum, the signal corresponding to the methylene carbon appears as a singlet at 78.7 ppm. The signal located at 93.2 ppm is assigned to the carbon atom which is bonded to the chlorine atoms.

Thermogravimetric and differential thermal analysis (TGA and DTA)

The TGA and DTA data for $CCl_3CH_2OSO_2NH_2$ are shown in Fig. 4. The TGA curve shows that the solid is stable up to 150 °C. The endothermic peak located at 58 °C in the DTA curve without mass loss in TGA corresponds to the melting point of the sample. The thermal decomposition of the substance takes place in three different steps. The first one ends at 188 °C with a mass loss of 11.62%. The DTA curve shows one exothermic peak located at 186 °C. The second step ends at 250 °C with 50.01% of mass loss. Three exothermic peaks located at 202, 211 and 242 °C are observed in the DTA. The mass loss observed in the temperature range of 250–500 °C is 29.20%. This decomposition step is associated with one endothermic peak with a DTA maximum at 368 °C. The three decomposition steps observed in the TGA and DTA curves could be attributed to the evolution of different volatile compounds such as SO_2, H_2O, N_2 and Cl_2.

The total mass loss from room temperature to 500 °C is 90.83%. This is in agreement with the theoretical mass loss calculated for the formation of carbon as final product (89.5%).

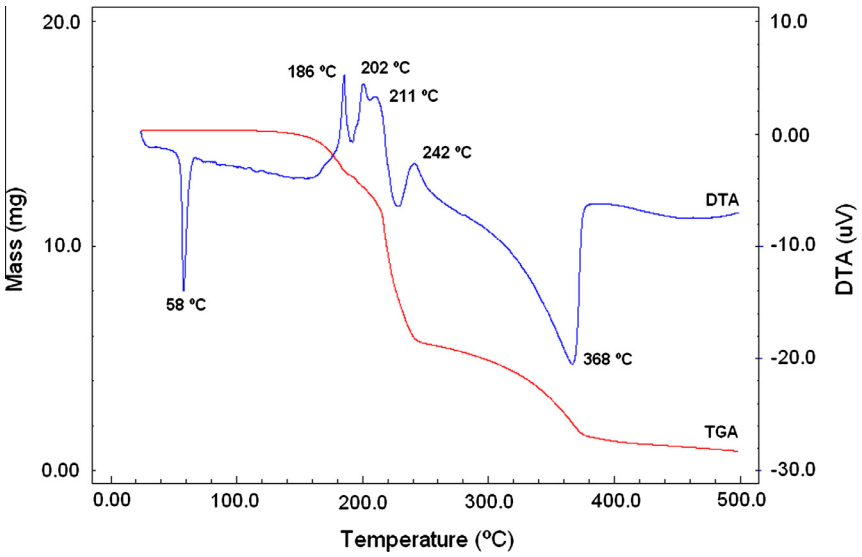

Fig. 4. TGA and DTA curves for $CCl_3CH_2OSO_2NH_2$.

Vibrational analysis

The assignment of the experimental infrared absorption and Raman dispersion bands to the normal modes of vibration of $CCl_3CH_2OSO_2NH_2$ was based on the comparison with related molecules [29–38] and assisted by the theoretical calculations performed in this work.

The solid state FTIR and Raman spectra and the simulated (SQM) spectra are compared in Figs. 5 and 6. The frequencies of the observed spectral features are collected in Table 5.

Infrared spectroscopy is an important auxiliary technique for quantitative conformational analysis. The C2 conformer is 1.37 kJ/mol higher in free energy at the B3LYP/6-311++G(d,p) method than the C1 conformer and at room temperature, C1 and C2 can be expected to be significantly populated. The conformationally averaged IR spectrum is obtained by summing the population-weighted spectra of C1 and C2 conformers calculated by using B3LYP/6-311++G(d,p) frequencies and intensities considering Lorentzian band shapes ($\gamma = 2\ cm^{-1}$). The populations are calculated from the B3LYP/6-311++G(d,p) energy difference via Boltzmann statistics and amount to 63% and 37%, respectively. It a

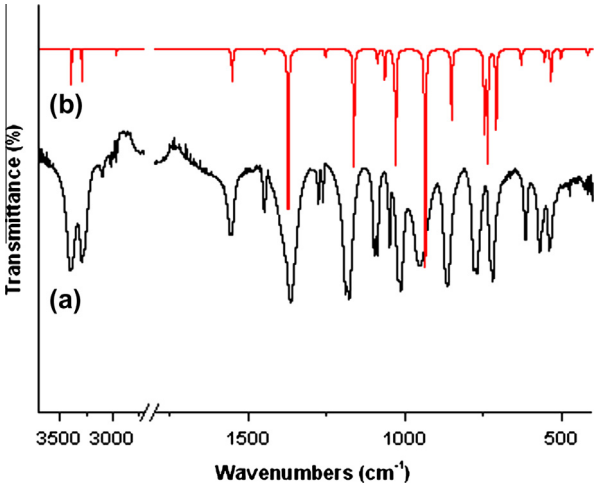

Fig. 5. Infrared absorption spectra of $CCl_3CH_2OSO_2NH_2$. (a) In solid state, resolution 2 cm^{-1}, and (b) simulated (SQM) spectrum.

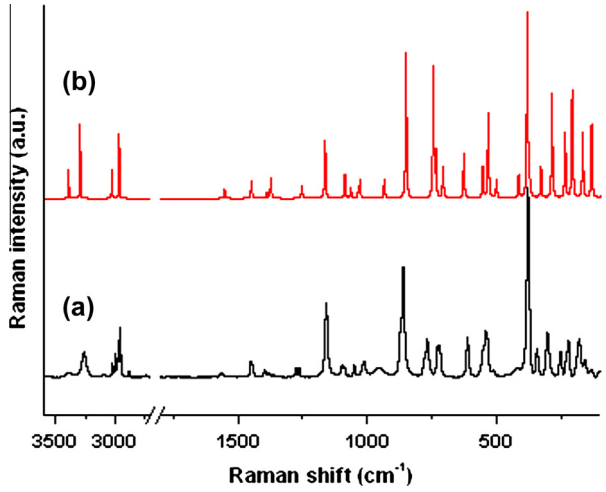

Fig. 6. Raman dispersion spectra (a) experimental, in the solid state, and (b) simulated.

conformationally averaged IR spectrum much closer to that of C1 than to that of C2 and leads straightforwardly to the assignment of the experimental spectrum shown in Fig. 5.

At room temperature, most of the bands are attributable to the same fundamental for both conformations. The IR and Raman spectra of the solid unambiguously demonstrate the presence of C1 and C2 conformers whose profiles have been simulated in Figs. 5 and 6. The predicted conformational splittings for the modes are in good agreement with the observed splitting in the solid infrared and Raman spectra. The vibrational analysis and force field have been performed only for the most stable conformer, which is C1. The B3LYP method has been chosen for the aforementioned analysis since it is the standard method for that purpose yielding, in general, reasonable results.

The B3LYP calculations reproduced the observed frequencies of the normal mode vibrations of $CCl_3CH_2OSO_2NH_2$ with the following root mean square deviation (RMSD) values for each basis set: 6-31G(d), 68.4 cm^{-1}; 6-311G(d,p), 62 $cm^{-1}$and 6-311++G(d,p), 66.6 cm^{-1}. However, the second and third basis sets reproduce the experimental frequencies somewhat better. The frequencies calculated with this method for the 36 normal modes of vibration

Table 5
Observed and calculated frequencies (in cm^{-1}), infrared and Raman intensities and potential-energy distribution (PED) for the conformer 1 of $Cl_3CCH_2OSO_2NH_2$.

Mode	Infrared[a] (solid)	Raman[a] (solid)	Calculated[a]	Calculated SQM[b]	IR intesity[c]	Raman activity[d]	Potential-energy distribution[e]	Approximate description of mode
1	3397 s	3394 (2)	3614	3391	57.16	46.32	100 S_1	ν_aNH_2
2	3293 s	–	3510	3294	50.70	112.33	100 S_2	ν_sNH_2
3	3020 w	3024 (8)	3133	3026	0.30	33.61	99 S_3	ν_aCH_2
4	2972 w	2973 (20)	3068	2965	11.27	74.28	99 S_4	ν_sCH_2
5	1554 m	1563 (2)	1592	1552	50.31	3.32	100 S_5	δNH_2
6	1449 w	1449 (8)	1487	1451	7.95	5.36	100 S_6	δCH_2
7	1396 sh	1396 (4)	1409	1393	1.19	1.54	92 S_7	ωCH_2
8	1365 vs	1362 (1)	1370	1373	251.13	6.05	99 S_8	ν_aSO_2
9	1276 w	1277 (5)	1285	1253	12.26	3.35	94 S_9	$\tau\omega CH_2$
10	1190 vs	–	1150	1175	180.1	13.61	86 S_{10}	ν_sSO_2
11	1098 s	1098 (8)	1102	1085	23.63	5.01	76 S_{11}	ρNH_2
12	1049 m	1050 (7)	1088	1071	46.87	2.32	39 S_{12} + 57 S_{14}	νC(1)—C(12)
13	1022 w	1021 (6)	1062	1035	24.06	1.17	84 S_{13}	ρCH_2
14	1013 m	1013 (8)	1025	1022	177.62	3.77	34 S_{14} + 43 S_{12}	νC(1)—O(3)
15	953 m	956 (5)	869	962	351.2	3.15	40 S_{15} + 19 S_{19} + 12 S_{21}	νS(6)—N(2)
16	864 m	862 (58)	821	844	106.85	22.94	24 S_{16} + 56 S_{17} + 21 S_{27} + 15 S_{30}	νS(6)—O(3)
17	780 m	782 (10)	717	783	121.73	17.16	45 S_{16} + 44 S_{17}	ν_aCCl_3
18	728 sh	729 (17)	700	738	176.83	5.31	66 S_{18} + 29 S_{19} + 10 S_{29}	ν_aCCl_3
19	720 m	720 (17)	662	721	133.8	4.16	38 S_{18} + 54 S_{19}	ωNH_2
20	616 w	614 (21)	599	624	22.11	4.71	29 S_{20} + 11 S_{25} + 15 S_{32}	ν_sCCl_3
21	570 w	–	517	563	20.89	3.07	48 S_{21} + 23 S_{22}	ωSO_2
22	558 sh	555 sh	505	537	51.76	7.46	23 S_{21} + 24 S_{22} + 29 S_{20}	δSO_2
23	474 vw	–	474	467	14.10	1.48	16 S_{23} + 44 S_{26}	ρSO_2
24	422 vw	423 (5)	401	416	10.97	1.38	68 S_{24} + 14 S_{26} + 24 S_{22}	δN—S—O
25	–	382 (100)	374	375	1.83	11.14	38 S_{25} + 26 S_{20}	δ_sCCl_3
26	–	346 (15)	364	347	3.77	2.01	25 S_{26} + 58 S_{23}	$\tau\omega SO_2$
27	–	306 (24)	347	331	2.24	1.72	12 S_{27} + 58 S_{33}	δO—C—C
28	–	256 (14)	294	279	1.10	4.49	33 S_{28} + 19 S_{23}	$\delta_{as}CCl_3$
29	–	232 sh	252	238	0.75	2.21	70 S_{29} + 17 S_{33}	$\delta_{as}CCl_3$
30	–	225 (19)	219	210	1.22	2.49	87 S_{30} + 26 S_{28} + 11 S_{23}	ρCCl_3
31	–	191 sh	216	202	19.23	1.06	55 S_{28} + 24 S_{31}	τNH_2
32	–	183 (20)	168	167	0.07	1.50	31 S_{32} + 20 S_{25}	ρCCl_3
33	–	132 (4)	141	135	4.38	1.32	12 S_{33} + 34 S_{34}	ρCCl_3
34	–	107 (3)	89	85	0.53	0.21	40 S_{27} + 29 S_{30} + 27 S_{34}	τS—O
35	–	–	46	–	3.08	0.05	–	τCCl_3
36	–	–	22	–	3.36	0.09	–	τC—O
RMSD (cm^{-1})			66.63	11.80				

[a]sh, shoulder; br, broad; s, strong; w, weak; m, medium; v, very. [b]Relative band heights in parentheses.
[a] B3LYP/6-311++G(d,p) calculation. Observed and calculated values in cm^{-1}.
[b] From scaled quantum mechanics force field (see text for further definition).
[c] Units are km mol^{-1}.
[d] Units are $Å^4$ $(amu)^{-1}$.
[e] Coordinate numbers correspond to Table S6 (Supplementary material).

of $CCl_3CH_2OSO_2NH_2$ (C_1 group) appear in Table 5 where they are compared with the measured ones. The IR and Raman spectra of the solid uncover the presence of C1 and C2 conformers through the splitting of several fundamental modes.

Assignment of bands

NH_2 group modes. The strong band located at 3399 cm^{-1} in the IR spectrum is assigned to the anti-symmetric stretching mode of the NH_2 group. Two bands, a strong one located at 3293 cm^{-1} and a shoulder at 3263 cm^{-1}, are assigned to the symmetric stretching vibration of the NH_2 group of C1 and C2 conformers, respectively. The Raman spectrum shows only two bands in this region, located at 3394 and 3263 cm^{-1}. This assignment was performed according to the characteristic wave numbers expected for this group. Table 6 shows wavenumbers of the vibrational modes of the $-SO_2NH_2$ moiety in 5-amino-1,3,4-thiadiazole-2-sulfonamide (Hats) [29], $CH_3SO_2NH_2$ [38], $CF_3SO_2NH_2$ [34] and $ClSO_2NH_2$ [36].

Two bands with medium intensity located at 1554 and 1548 cm^{-1} in the IR and Raman spectra, respectively, are assigned to the NH_2 deformation.

The weak features at 1098 and 1088 cm^{-1} in the IR and Raman spectrum are assigned to the rocking vibration of the NH_2 group for C1 and C2, respectively. This assignment is in agreement with the calculated wavenumbers. The band located at 720 cm^{-1} is assigned to the wagging mode in agreement with the values reported by related molecules [29,30,35–38], except in $CF_3SO_2NH_2$ where the value reported for this vibration is 430 cm^{-1} [34].

SO_2 group modes. The SO_2 anti-symmetric and symmetric stretching modes appear in the region between 1390 and 1300 cm^{-1} and 1182 and 1140 cm^{-1}, respectively, in different related molecules [29–38]. The very intense IR absorption band observed at 1365 cm^{-1} is assigned to the anti-symmetric stretching mode. This mode appears in the Raman spectrum as a dispersion band with medium intensity at 1362 cm^{-1}. Two intense bands appear in the IR spectrum at 1190 and 1178 cm^{-1}. These bands are assigned to the symmetric stretching mode. These results are in agreement with the calculated ones. These bands appear split in the IR spectrum hence showing the presence of both conformers in the sample. The Raman spectrum shows only a single band located at 1160 cm^{-1} corresponding to this mode. We have observed

Table 6
Vibrational modes frequencies (cm^{-1}) of the $—SO_2NH_2$ moiety in $CCl_3CH_2OSO_2NH_2$ and in related molecules such as 5-amino-1,3,4-thiadiazole-2-sulfonamide (Hats), $CH_3SO_2NH_2$, $CF_3SO_2NH_2$ and $ClSO_2NH_2$.

Vibrational mode	$CCl_3CH_2OSO_2NH_2$[a]	Hats[b]	$CH_3SO_2NH_2$[c]	$CF_3SO_2NH_2$[d]	$ClSO_2NH_2$[e]
ν_aNH_2	3399	3307	3320	3392	3386
ν_sNH_2	3293, 3263	3172	3245	3280	3282
δNH_2	1554	1580	1576	1522	1548
ν_aSO_2	1365	1342	1315	1357	1383
ν_sSO_2	1178	1140	1145	1153	1182
ρNH_2	1098, 1088	1097	1166	1046	1068
ωNH_2	720	636 (calc.)	689	432	688
ωSO_2	570	584	493	628	588
δSO_2	558	500	533	495	508
$\tau\omega SO_2$	346	315	345 (calc.)	394 (calc.)	430
$\nu S—N$	953	944	881	957	921
τNH_2	191	157	430	306 (calc.)	313

[a] This work.
[b] Ref. [29].
[c] Ref. [38].
[d] Ref. [34].
[e] Ref. [36].

a difference between the observed and calculated wavenumber values of the symmetric stretching mode because C1 and C2 conformers are arranged in the lattice as center-symmetric N—H···O(sulf)-bonded dimers and this mode is very sensitive to intermolecular interactions.

The IR shoulder observed at 558 cm^{-1} is assigned to the SO_2 bend. This wavenumber is somewhat higher than usual, as this mode appears in the region between 533 and 495 cm^{-1} in the compounds listed in Table 6. The bands of the three modes corresponding to the whole SO_2 group appear at relatively low wavenumbers and the following assignment is proposed: 570 cm^{-1} (SO_2 wagging), 474 cm^{-1} (SO_2 rocking) and 346 cm^{-1} (SO_2 twisting). These assignments are also supported by quantum chemical calculations.

Methylene group modes. The weak IR bands at 3020 and 2996 cm^{-1} are assigned to the CH_2 anti-symmetric stretching mode for C1 and C2 conformers, respectively. These bands appear at 3024 and 2995 cm^{-1} in the Raman spectrum. The bands corresponding to the CH_2 symmetric stretching mode appear in the IR spectrum as weak bands located at 2972 and 2954 cm^{-1} and as medium intensity bands at 2973 and 2955 cm^{-1} in the Raman spectrum. They appear split, again indicating the presence of the two conformers.

The bands located at 1449 and 1446 cm^{-1} in the IR spectra (1449 and 1443 cm^{-1} in the Raman spectrum) are assigned to the CH_2 bending mode of both conformers. The bands corresponding to the wagging and twisting of both conformers are observed at 1396 and 1276 cm^{-1}. The weak band observed at 1022 cm^{-1} in the IR and Raman spectra is assigned to the rocking mode.

Trichloromethyl group modes. The assignment of the bands corresponding to CCl_3 group was made by comparison and with the corresponding ones of the $ClC(O)CCl_3$ molecule [39] and with quantum chemical calculations.

The two medium-intensity absorption bands observed at 780 and 770 cm^{-1} and the shoulder located at 728 cm^{-1} in the IR spectrum are assigned to the CCl_3 anti-symmetric stretching modes, which are calculated at 717 and 700 cm^{-1} in the theoretical spectrum. The strongest band in the Raman dispersion spectrum of the solid, at 382 cm^{-1} is assigned to the CCl_3 symmetric deformation, which is theoretically predicted at 374 cm^{-1}. In $ClC(O)CCl_3$ the band appears at 411 cm^{-1}.

According to the theoretical calculations, the CCl_3 symmetric stretching mode is assigned to the band located at 616 cm^{-1} in the IR spectrum. This band appears at 590 cm^{-1} in $ClC(O)CCl_3$. The two bands observed in the Raman spectrum at 256 and 231 cm^{-1} are assigned to the CCl_3 anti-symmetric bending. The band corresponding to the rocking of CCl_3 is observed in the Raman spectrum at 183 and 136 cm^{-1}.

Skeletal modes. The C—O stretching mode appears as a medium-intensity band in both the IR and Raman spectra at 1013 cm^{-1}. The medium-intensity band located at 1049 cm^{-1} is assigned to the C—C stretching vibration as indicated by our calculated value of 1089 cm^{-1}. The S—O stretching mode is usually strongly mixed with other vibrations, but in this case it appears as a strong dispersion band in the Raman spectrum located at 862 cm^{-1} (864 cm^{-1} in the IR spectrum).

The ν(S—N) mode gives rise to a band of weak-to-moderate intensity in the range 960–880 cm^{-1}. The S—N stretching mode exhibits a medium-intensity IR absorption band located at 953 cm^{-1} and a weak Raman band at 956 cm^{-1}. Theoretically we have obtained for to this mode a value of 869 cm^{-1}. Presumably, the position of this band could be explained by the degree of conjugation present in the molecule. Similar high wavenumbers for this mode are reported for different molecules as appreciated in Table 6.

The very weak IR band observed at 422 cm^{-1} is assigned to the NSO bending mode. This value is close to the one predicted by theoretically (401 cm^{-1}). The OCC bending mode appears as a Raman band located at 306 cm^{-1}. This value is close to the one predicted Tuttolomondo et al. for $CF_3SO_2OCH_2CH_3$ (359 cm^{-1}) [40].

Torsional modes. The shoulder located at 191 cm^{-1} in the Raman spectrum is assigned to the NH_2 torsion. This value is similar to the corresponding one reported by Hats [29] but lower than the values reported for $CF_3SO_2NH_2$ [34], $ClSO_2NH_2$ [36] and $CH_3SO_2NH_2$ [38]. The weak Raman band located at 107 cm^{-1} is assigned to the torsion around the S—O bond, as this observed wavenumber is close to the value calculated for this mode. The dispersion band expected for the torsion mode around the C—O bond could not be observed in our Raman spectra.

Calculation of force constants

The Cartesian force field resulting from the B3LYP/6-311++G(d,p) calculation for both conformers of $CCl_3CH_2OSO_2NH_2$ was transformed to the set of non-redundant natural internal coordinates defined in Table S6. Such coordinates take into account the local symmetry around the C-atoms and follow the proposal of Fogarasi et al. [41]. The force field obtained was subsequently

Table 7
Force constants in internal (valence) coordinates for C1 and C2 conformers of $Cl_3CCH_2OSO_2NH_2$ and related molecules.

Force constants[a]	$Cl_3CCH_2OSO_2NH_2$[b,*]		$CF_3SO_2NH_2$[c]	$CF_3SO_2OCH_2CH_3$[d]	$CF_3SO_2OCCl_3$[e]
	Conformer 1	Conformer 2			
k_f [N(2)—H]	6.204	6.196	6.19	–	–
k_f [N(2)—S(6)]	5.287	5.288	6.23	–	–
k_f [S=O]	10.18	10.18	10.17	10.73	11.0
k_f [S—O]	4.532	4.532	–	5.04	3.78
k_f [C—O]	4.966	4.966	–	4.20	4.45
k_f [C—C]	3.853	3.853	–	4.27	–
k_f [C—H](CH_2)	4.943	4.874	–	4.90	–
k_f [C(12)—Cl(7,14)]	3.411	3.411	–	–	3.46
k_f [C(12)—Cl(13)]	3.562	3.562	–	–	–
k_f [O=S=O]	1.261	1.261	1.11	1.14	0.96
k_f [O—S=O]	1.311	1.311	–	1.27	1.13
k_f [N—S=O]	1.311	1.311	1.30	–	–

[*] Calculated at the B3LYP/6-311++G(d,p) level.
[a] Units are mdyn $Å^{-1}$ for stretches and stretch–stretch interactions and mdyn Å rad^{-2} for angle bends.
[b] This work.
[c] Ref. [43].
[d] Ref. [40].
[e] Ref. [44].

scaled using the scheme proposed by Pulay et al. [42]. Initial scale factors were assumed to be equal to one for all modes and they were subsequently modified by a least-squares procedure to obtain the best fit to the experimental wave numbers, as shown in Table S7. During the refinement, the same weight was assigned to all vibration wavenumbers and no empirical correction was used for the theoretical geometry. The resulting scaled quantum mechanical (SQM) force field was then used to calculate the potential energy distribution of the molecule. The final RMSD and potential energy distribution are shown in Table 5. The internal force constants were calculated with the SQM force field and the results are shown in Table 7 where they are compared with equivalent values for related molecules. For conformer 1 it was observed a value of k_f [N(2)—H] higher than the corresponding one calculated for the conformer 2. This could be explained by the fact that LP O(3) → σ* S(6)—N(2) interaction is higher in C1 than in C2 (see Table 2). This effect produces a lengthening of the S—N bond and an increase of the force constant for the N—H bond. Another difference in both conformers was observed in the force constants of the C—H bond corresponding to the methylene groups. In C1 the k_f [C(1)—H] is higher than in C2 due to the higher LP O(3) → σ* C(1)—H interaction as compared with C2.

The calculated S—N bond length turns out to be shorter in $CF_3SO_2NH_2$ [43] as compared with $CCl_3CH_2OSO_2NH_2$ (1.671 and 1.677 Å) and, consequently, the corresponding force constant increases from 5.28 mdyn $Å^{-1}$ in $CCl_3CH_2OSO_2NH_2$ to 6.23 mdyn $Å^{-1}$ in $CF_3SO_2NH_2$. This behavior is in agreement with the observed increase in the frequency of the S—N stretching mode (see Table 6). The adjacent S—O bond length increases in the order $CF_3SO_2OCH_2$-CH_3 (1.610 Å) < $CCl_3CH_2OSO_2NH_2$ (1.632 Å) < $CF_3SO_2OCCl_3$ (1.690 Å) [44]. This agrees with the decrease of the S—O force constants following this same order.

In $CCl_3CH_2OSO_2NH_2$ we observe a force constant for the C(1)—O(3) stretching mode of 4.97 mdyn $Å^{-1}$. This value indicates that the C—O bond is strengthened by the presence of the —CCl_3 group which is an excellent leaving group for different chemical reactions that involve the transference of this group.

Conclusions

The crystal and molecular structure of 2,2,2-trichloroethoxysulfonamide, $CCl_3CH_2OSO_2NH_2$, has been disclosed by X-ray diffraction methods and the gas phase structure calculated by quantum chemistry. The substance crystallizes in the monoclinic $P2_1/c$ space group with $a = 9.969(3)$ Å, $b = 22.914(6)$ Å, $c = 7.349(2)$ Å, $\beta = 91.06(3)°$, and $Z = 8$ molecules per unit cell. There are two independent but closely related molecular conformers in the crystal asymmetric unit. They only differ in the angular orientation of the sulfonamide (—SO_2NH_2) group. The conformers are arranged in the lattice as center-symmetric N—H···O(sulf)-bonded dimers. Neighboring dimers are linked through further N—H···O(sulf) bonds giving rise to a crystal layered structure.

The thermal behavior of the substance showed that the solid was stable up to 150 °C and the melting point was 58 °C. The thermal decomposition of this compound takes place in three different steps with a total mass loss of 90.83%.

According to NBO analysis, the hyper-conjugative interactions are more favored in conformer 2 than in conformer 1. These results were confirmed by AIM analysis.

Infrared absorption and Raman dispersion spectra of solid state $CCl_3CH_2OSO_2NH_2$ showed bands assignable to 34 of the 36 expected normal modes of vibrations. It was possible to scale the theoretical force field by using the observed frequencies. The resulting SQM force field was employed to calculate the potential energy distribution, which revealed the physical nature of the fundamental vibration modes and the force constants in terms of internal coordinates of the compound. The force constant values for $CCl_3CH_2OSO_2NH_2$ are in agreement with the values reported for related molecules and show that the compound could be used as a reactive for the transference of CCl_3 groups in different chemical reactions.

Acknowledgments

This work was supported by CIUNT and CONICET (PIP 1529), and by ANPCyT (PME06 2804 and PICT06 2315) of Argentina. D.M.G. is recipient of a postdoctoral fellowship from CONICET. Authors thank Mr. M. Arias for Raman spectra measurements.

Appendix A. Supplementary material

Supplementary data associated with this article can be found, in the online version, at http://dx.doi.org/10.1016/j.saa.2013.07.013.

References

[1] A. Scozzafava, T. Owa, A. Mastrolorenzo, C.T. Supuran, Curr. Med. Chem. 10 (2003) 925.
[2] C.T. Supuran, A.J. Scozzafava, Enzyme Inhib. Med. Chem. 15 (2000) 597.
[3] K. Williams Fiori, J. Du Bois, J. Am. Chem. Soc. 129 (2007) 562.
[4] Q. Xu, D.H. Appella, Org. Lett. 10 (2008) 1497.

[5] CrysAlisPro, Oxford Diffraction Ltd., version 1.171.33.48 (release 15-09-2009 CrysAlis171.NET).
[6] G.M. Sheldrick, SHELXS-97. Program for Crystal Structure Resolution, University of Göttingen, Göttingen, Germany, 1997.
[7] G.M. Sheldrick, Acta Crystallogr. A 46 (1990) 467.
[8] G.M. Sheldrick, SHELXS-97. Program for Crystal Structure Analysis, University of Göttingen, Göttingen, Germany, 1997.
[9] G.M. Sheldrick, Acta Crystallogr. A 64 (2008) 112.
[10] National Service for Computational Chemistry Software (NSCCS), <http://www.nsccs.ac.uk>.
[11] M.J. Frisch, J.A. Pople, J.S. Binkley, J. Chem. Phys. 80 (1984) 3265;
M.J. Frisch, J.A. Pople, J.S. Binkley, J. Chem. Phys. 80 (1984) 3265. M.J. Frisch, G.W. Trucks, H.B. Schlegel, G.E. Scuseria, M.A. Robb, J.R. Cheeseman, J.A. Montgomery, Jr., T. Vreven, K.N. Kudin, J.C. Burant, J.M. Millam, S.S. Iyengar, J. Tomasi, V. Barone, B. Mennucci, M. Cossi, G. Scalmani, N. Rega, G.A. Petersson, H. Nakatsuji, M. Hada, M. Ehara, K. Toyota, R. Fukuda, J. Hasegawa, M. Ishida, T. Nakajima, Y. Honda, O. Kitao, H. Nakai, M. Klene, X. Li, J.E. Knox, H.P. Hratchian, J.B. Cross, C. Adamo, J. Jaramillo, R. Gomperts, R.E. Stratmann, O. Yazyev, A.J. Austin, R. Cammi, C. Pomelli, J.W. Ochterski, P.Y. Ayala, K. Morokuma, G.A. Voth, P. Salvador, J.J. Dannenberg, V.G. Zakrzewski, S. Dapprich, A.D. Daniels, M.C. Strain, O. Farkas, D.K. Malick, A.D. Rabuck, K. Raghavachari, J.B. Foresman, J.V. Ortiz, Q. Cui, A.G. Baboul, S. Clifford, J. Cioslowski, B.B. Stefanov, G. Liu, A. Liashenko, P. Piskorz, I. Komaromi, R.L. Martin, D.J. Fox, T. Keith, M.A. Al-Laham, C.Y. Peng, A. Nanayakkara, M. Challacombe, P.M.W. Gill, B. Johnson, W. Chen, M.W. Wong, C. González, J.A. Pople, Gaussian 03, Revision C.02, Gaussian, Inc., Wallingford, CT, 2004.
[12] C. Møller, M.S. Plesset, Phys. Rev. 46 (1934) 618.
[13] R. Krishnan, J.S. Binkley, R. Seeger, J.A. Pople, J. Chem. Phys. 72 (1980) 650.
[14] A.D. McLean, G.S. Chandler, J. Chem. Phys. 72 (1980) 5639.
[15] M.J. Frisch, J.A. Pople, J.S. Binkley, J. Chem. Phys. 80 (1984) 3265.
[16] W.J. Hehre, P.V.R. Schleyer, J.A. Pople, Ab Initio Molecular Orbital Theory, Wiley, New York, 1986.
[17] A.D. Becke, J. Chem. Phys. 98 (1993) 5648.
[18] C. Lee, W. Yang, R.G. Parr, Phys. Rev. B 37 (1988) 785.
[19] C. Alamo, B. Barone, J. Chem. Phys. 108 (1998) 664.
[20] E.D. Glendening, J.K. Badenhoop, A.D. Reed, J.E. Carpenter, F.F. Weinhold, Theoretical Chemistry Institute, University of Wisconsin, Madison, WI, 1996.
[21] R.F.W. Bader, Atoms in Molecules, A Quantum Theory, Claredon press, Oxford, 1990.
[22] F. Biegler-Köning, J. Schönnbohn, D. Bayles, J. Comput. Chem. 22 (2001) 545.
[23] W.B. Collier, Program FCARTP (QCPE #631), Department of Chemistry, Oral Roberts University, Tulsa, OK, 1992.
[24] B. Nielsen, A.J. Holder, GaussView, User's Reference, Gaussian Inc., Pittsburgh, PA, 1997–1998.
[25] C.K. Johnson, ORTEP II. A Fortran Thermal-Ellipsoid Plot Program. Report ORNL-5318, Oak Ridge National Laboratory, Tennessee, USA, 1976.
[26] K. Sarojini, H. Krishan, C. Kanakam, S. Muthu, Spectrochim. Acta A 96 (2012) 657.
[27] G. Cami, E. Chacón Villalba, E. Di Santi, P. Colinas, G. Estiu, D.B. Soria, J. Mol. Struct. 995 (2011) 72.
[28] G. Cami, E. Chacón Villalba, P. Colinas, G.A. Echeverria, G. Estiu, D.B. Soria, J. Mol. Struct. 1024 (2012) 110.
[29] G. Cami, E.E. Chufán, J.C. Pedregos, E.L. Varetti, J. Mol. Struct. 570 (2001) 119.
[30] H.T. Varguese, C.Y. Panicker, D. Philip, Spectrochim. Acta A 65 (2006) 155.
[31] M.E. Tuttolomondo, A. Navarro, T.P. Ruiz, E.L. Varetti, S.A. Hayes, D.A. Wann, H.E. Robertson, D.W. Rankin, A. Ben Altabef, J. Phys. Chem. A 111 (2007) 9952.
[32] M.E. Tuttolomondo, P.E. Argañaraz, E.L. Varetti, S.A. Hayes, D.A. Wann, Robertson H.E. Robertson, D.W. Rankin, A. Ben Altabef, Eur. J. Inorg. Chem. (2007) 1381.
[33] A. Borba, A. Gómez-Zavaglia, R. Fausto, J. Phys. Chem. A 117 (2013) 704.
[34] L.E. Fernández, A. Ben Altabef, A.C. Fantoni, E.L. Varetti, Spectrochim. Acta A 53 (1997) 189.
[35] H.M. Badawi, Spectrochim. Acta A 65 (2006) 453.
[36] R.M.S. Alvarez, E.H. Cutín, H.G. Mack, C.O. Della Védova, J. Mol. Struct. 440 (1998) 213.
[37] R.M.S. Alvarez, M.I. Mora Valdez, E.H. Cutin, C.O. Della Védova, J. Mol. Struct. 657 (2003) 291.
[38] K. Hanai, T. Okuda, T. Uno, K. Machida, Spectrochim. Acta A 31 (1975) 1217.
[39] V.B. Arce, C.O. Della Védova, A.J. Downs, S. Parsons, R.M. Romano, J. Org. Chem. 71 (2006) 3423.
[40] M.E. Tuttolomondo, A. Navarro, E.L. Varetti, A. Ben Altabef, J. Raman Spectrosc. 36 (2005) 427.
[41] G. Fogarasi, X. Zhou, P.W. Taylor, P. Pulay, J. Am. Chem. Soc. 114 (1992) 8191.
[42] P. Pulay, G. Fogarasi, G. Pongor, J.E. Boggs, A. Braga, J. Am. Chem. Soc. 105 (1983) 7037.
[43] L.E. Fernández, A. Ben Altabef, E.L. Varetti, J. Mol. Struct. 612 (2002) 1.
[44] M.E. Defonsi Lestard, L.A. Ramos Guerrero, M.E. Tuttolomondo, S.E. Ulic, A. Ben Altabef, Vib. Spectrosc. 55 (2011) 153.